BULLETIN OF THE POLISH ACADEMY OF SCIENCES
TECHNICAL SCIENCES, Vol. 70(6), 2022, Article number: e143827
DOI: 10.24425/bpasts.2022.143827

Metrological analysis of additively manufactured copies of a fossil skull

Miroslaw RUCKI[1]*, Yaroslav GARASHCHENKO[2], Ilja KOGAN[3,4], and Tomasz RYBA[5]

[1] Faculty of Mechanical Engineering, Kazimierz Pulaski University of Technology and Humanities in Radom, Poland
[2] Department of Integrated Technologic Process and Manufacturing, National Technical University "Kharkiv Polytechnic Institute", Ukraine
[3] Museum für Naturkunde Chemnitz, Germany
[4] Geological Institute, TU Bergakademie Freiberg, Germany
[5] Łukasiewicz Research Network – Institute for Sustainable Technologies, Radom, Poland

Abstract. This paper presents the results of a metrological analysis of the additively manufactured (AM) copies of a complex geometrical object, namely the fossil skull of *Madygenerpeton pustulatum*. This fossil represents the unique remains of an extinct "reptiliomorph amphibian" of high importance for palaeontological science. For this research, the surface was scanned and twelve different copies were 3D-printed using various devices, materials, and AM techniques. The same digitized model was used as a reference to compare with the surfaces obtained by Mitutoyo Coordinate Measuring Machine (CMM) CRYSTA-Apex S 9166 for each copy. The fidelity of the copies was assessed through statistical analysis of the distances between compared surfaces. The methodology provided a good background for the choice of the most accurate copies and the elimination of the less accurate ones. The proposed approach can be applied to any object of complex geometry when reproduction accuracy is to be assessed.

Key words: additive manufacturing; *Madygenerpeton*; optical measurement; statistical analysis.

1. INTRODUCTION

While 3D scanning and additive manufacturing (AM) reproduction became standard techniques in archaeology, very few reports can be found concerning AM application in palaeontology. The objective of this paper is to assess the fidelity of the 3D-printed models of a natural complex geometrical object with no initial documentation, fabricated using different AM technologies. The object of interest is a fossil skull of a "reptiliomorph amphibian" *Madygenerpeton pustulatum* [1] from the Triassic of Madygen in Kyrgyzstan (Central Asia). This unique find constitutes the holotype of the species, i.e. the specimen on which the species has been defined and with which new finds and similar animals have to be compared. The importance of a holotype demands that specific measures of preservation and security be applied to it. Usually, holotypes are kept in protected repositories with access only for visiting scientists or sometimes displayed on exhibitions. They are not normally given out on loan nor sent abroad or shown to students in regular lectures. At the same time, interest in such specimens in the frame of scientific comparative analysis on a broader scale, palaeontological education or the promotion of geoheritage requires their accessibility to a wide range of colleagues, students and the general public. Traditionally, fossil specimens have been replicated using molds. However, this process is time-consuming and, critically, bears the risk of damaging the original during manipulations with adhesive resin. The development of digital technologies allows for capturing and replicating three-dimensional objects while avoiding contact and minimizing manipulation of the original. Thus, the damage risk is reduced, and since there are no limitations to the number of replicas, the range of their availability can be dramatically widened. Apart from high-fidelity scientific copies and high-quality exhibition objects, models at original, enlarged or diminished scale can be prepared for training or merchandise purposes and optimized for the needs of visitors with disabilities.

AM technologies offer numerous possibilities to fabricate objects of complex geometry and manifold shape [2]. These are relatively new methods using an incremental layer-by-layer materialization of a digital model. The AM methods referred to also as 3D printing (3DP), rapid prototyping (RP), or solid-freeform (SFF) became an exponentially evolving manufacturing technology [3]. The estimated average global value of the 3D printing market is recording a 25% year-to-year increase since 2014 and is expected to reach 35.0 billion USD by 2024 [4]. A good review of these methods can be found in [5], as well as in more recent works related to Industry 4.0 and Internet of Things concepts [6, 7]. It is emphasized that the cost of AM is a crucial factor [8]. There are also works that discuss design principles, constraints, and optimization for AM techniques [9].

At present, a large variety of individual additive processes are available depending on the material and machine technol-

*e-mail: m.rucki@uthrad.pl

Manuscript submitted 2022-06-10, revised 2022-09-17, initially accepted for publication 2022-10-19, published in December 2022.

ogy, which can be classified into seven main categories: material jetting, binder jetting, vat photopolymerization, material extrusion, powder bed fusion, sheet lamination, and direct energy deposition [10]. AM allows for hybrid- and multi-material (MM) manufacturing of metals and is especially suitable for functionally graded materials (FGMs) [11]. There are well-established and rapidly emerging applications of AM technologies far beyond the initial intent of prototyping, such as medical applications or direct digital manufacturing [12]. An increasing number of new applications also include palaeontological fossil specimens [13, 14].

From the literature review, it can be concluded that some of the main directions of 3D-printing development are geometry and material design for AM, computational tools and interface development, as well as manufacturing tools and process development [15]. In most published research papers, attention is paid to the optimization tasks of AM-process planning [16], CAD-AM (RP) programs [17], choice of AM technologies [18], the synthesis principles applied during the manufacturing process [19], design of cladding layers, the proper choice of building materials, including finally obtained surface quality [20], dimensional accuracy [21], as well as microstructural features [22].

2. MATERIALS AND METHODS

2.1. Research object

The replicated object is the holotype of *Madygenerpeton pustulatum* [1], an incomplete fossil skull that was recovered in 2007 from Madygen in southwest Kyrgyzstan [23]. Due to the international significance of the fossil deposit and further objects of geological heritage in the Madygen area, it is currently developed as a national geopark, with the prospect of inclusion into the UNESCO Global Geopark network. Geoscientific research conducted in the region since the first half of the 20th century has led to the discovery of the world's arguably richest non-marine fossil locality for the mid-Triassic age, dated to ca. 237 million years before the present. The assemblage comprises abundant and well-preserved remains of various aquatic and terrestrial plants, aquatic invertebrates, insects, fishes, and tetrapods with the investigated *Madygenerpeton pustulatum* among them, as well as trace fossils. It preserves one of the most complex and rich ecosystems documenting a crucial period in Earth's history that witnessed the origin of dinosaurs and the onset of modern biodiversity. In this context, it is crucial to present scientific results and accurate reconstructions of extinct animals, their morphology, ecology, and systematic interrelationships to a broad audience. At the same time, educational and scientific purposes require maximal fidelity in reproducing anatomical details.

The examined *Madygenerpeton pustulatum* belongs to Chroniosuchia. This is an extinct group of derived amphibians close to the origin of all higher vertebrates (mammals and reptiles including birds). It was a crocodile-like apex predator in the Madygen ecosystem described above. It is known from postcranial remains of at least three individuals and the single skull. This unique skull shown in Fig. 1a, somewhat deformed by fossilization processes and lacking the lower jaw, is the object of the present research. The bony surface of the skull is covered by sub-mm tubercles seen in Fig. 1b, which makes it an ideal object for studies on the possibilities and limitations of digital reproduction.

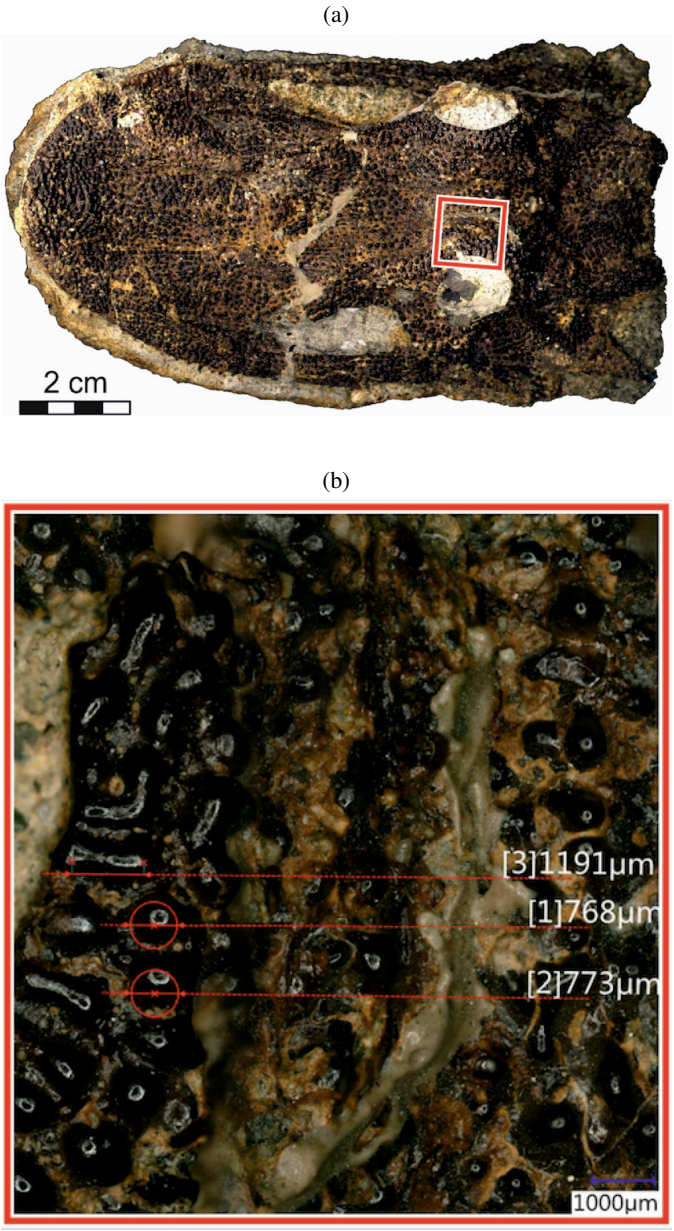

Fig. 1. Fossil skull of *Madygenerpeton pustulatum* (holotype FG 596/V/4, housed at the TU Bergakademie Freiberg): (a) general view, and (b) close-up picture of surface morphology

Two plaster casts produced from a silicone mold formed using one of the printed copies are shown in Fig. 2. Besides obvious deviations in geometry, none of them reproduces the fine surface structure with reasonable accuracy. Irregular blisters caused by air bubbles negatively affect the appearance. Finally, the creation of a 3D copy by this method would require the preparation of complex molds reflecting both sides of the fossil and a system ensuring form stability.

Fig. 2. Two plaster casts of the *Madygenerpeton pustulatum* fossil skull

2.2. Preparation of the 3D digital model

The final accuracy of the additively manufactured object with respect to the original depends not only on the AM technique, material and process parameters but above all on the digital model used. In the case of a unique object with no reference surface and unknown light-reflecting characteristics, digitization was a challenging task. To solve the problem, 3D digitization of the skull was performed with eight different devices and the obtained 3D models underwent comparative analysis between one another in two subsequent stages.

First, each pair of 3D digital models underwent visual and statistical analysis to assess the differences between them. Next, using geometrical and dimensional criteria, the closest fitting models were chosen. Finally, the distances Δ_d between surface polygons (triangles) were analyzed in detail statistically. The main statistical parameters included average (mean) values $\overline{\Delta_d}$, the maximal distances $\{\Delta d\}_{\max}$, and the standard deviations $\sigma\{\Delta_d\}$ between the respective polygons of the compared digital models [24].

After the rating was made, it was found that the digitization with AICON SmartScan exhibited the lowest distances to the models obtained from other scanners. However, for the 3D printing of the copies, the Artec Space Spider digitized model was chosen. It was third place in the rating, and, therefore, of high accuracy. Moreover, it was advantageous for practical reasons, namely, it provided a better, detailed geometry of the smallest elements of the fossil skull. As a result, the digitized "Artec surface model" was 20,978.512 mm^2, which was 11.8% larger than that obtained from the AICON device. Thus, the reference digital surface in this research was the model obtained from scanning the fossil skull with the Artec Space Spider device.

The obtained results provided the ground for rating the models according to their respective accuracies. In this way, one of the models was chosen for subsequent 3D-printing of the fossil skull copies and served as a reference in the present study, when the accuracy of these copies was assessed. The entire procedure is presented schematically in Fig. 3, and the 3D printing techniques, measurements method and fidelity assessment approach are described below.

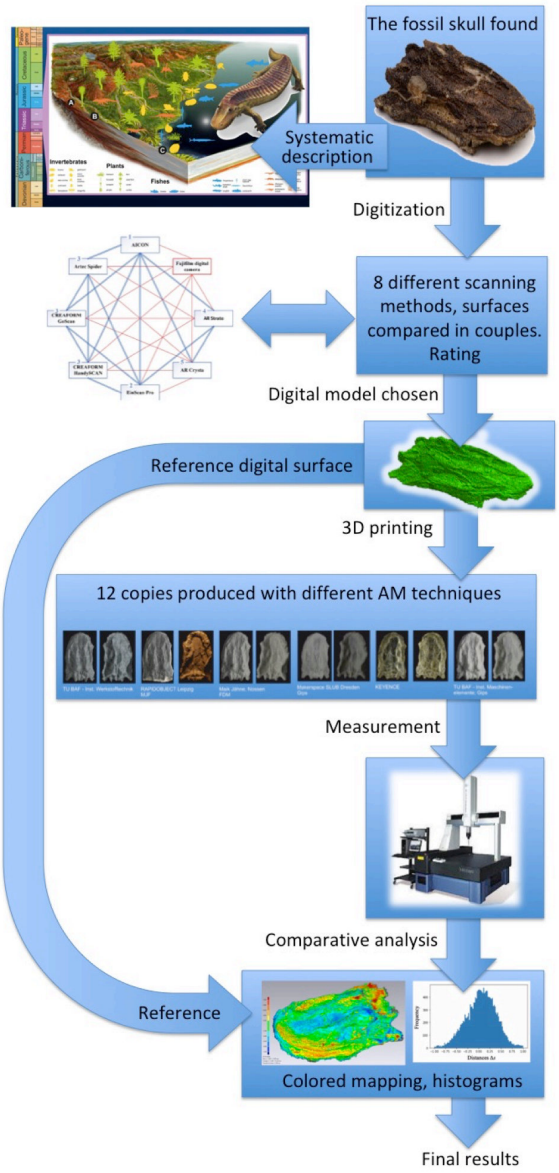

Fig. 3. Block diagram of the research procedure

2.3. Test campaign

To reach the main objective of the present research, the following steps were undertaken:

- Preparation of the 3D-printed copies of the object using the same digital model (later used as a reference), but different AM techniques.
- Scanning of the physical copies of the object to obtain their digital representations.
- Visual and statistical analysis of the differences between each representation and the reference digital model.
- Detailed statistical analysis of the differences in order to determine peculiarities of the applied AM methods and to point out the most suitable one for the investigated *Madygenerpeton* fossil skull.

Thus, based on the rating of the digital models [25], one of them was chosen for Additive Manufacturing. The same "Artec surface model" was used later as a reference surface in the metrological analysis. Next, 12 physical copies of the object were 3D-printed using a wide range of available AM techniques. Table 1 shows the main data of the devices and parameters used in experiments.

Table 1
Technologies and devices used for manufacturing the fossil skull copies [26]

Copy No.	Technologies	Equipment model	Material	Layer thickness, mm
#1	Extrusion-based FDM	Ultimaker 2+	PLA	0.100
#2	Multijet Fusion	HP Jet Fusion 3D 4210	Polyamid PA 12-HP	0.080
#3	Extrusion-based FDM	Prusa i3 MK2	PLA	0.050
#4	Powder-based 3D printing with inkjet	Canon ProJet 460Plus	White gypsum	0.125
#5	UV-resin-Inkjet	Continuous Inkjet Printers Keyence	Yellowish transparent	0.100
#6	Powder-based 3D printing with inkjet	ZCorp 310(R)	Gypsum, ZP151	0.088
#7	Powder-based 3D printing with inkjet	ZCorp 310(R)	Apricot kernel flour	0.088
#8	Polyjet	Stratasys J55	Standard material	0.019
#9	Polyjet	Stratasys J55	Vivid material	0.019
#10	ColorJet printing	3D Systems ProJet CJP 460Plus	VisiJet PXL	0.100
#11	ColorJet printing	3D Systems Zprinter 650	VisiJet PXL	0.089
#12	UV-curable inkjet printing	Mimaki 3DUJ-553	SW-100	0.032

2.4. Measurement

The 3D-printed copies were then scanned with a Mitutoyo Coordinate Measuring Machine (CMM) CRYSTA-Apex S 9166 at Mitutoyo Polska, Wrocław. The maximum permissible error of the CMM was $MPE_E = \pm(1.7 + 3L/1000)$ µm, where L is the measured length [mm]. The CMM was equipped with a temperature compensation system to guarantee measurement accuracy under different temperature conditions from 16 to 26°C Thermal compensation is applied based on 20°C

The surface scanning was performed with a non-contact line laser probe SurfaceMeasure 606 with a scanning error of 12 µm [1σ/sphere fit]. The automatic configuration of the camera sensitivity and the laser intensity settings were suitable to the environment and scanned materials with no need for powder or spray application. The accuracy of the CRYSTA-Apex CMM with this probe was found to be satisfactory after preliminary analysis [27]. The scanning procedure was performed in a single fixation in order to minimize the error generated by the formation of a points cloud. It should be noted, however, that copy #5 did not undergo optical scanning due to its transparency. At this stage of the research, it was excluded from the metrological analysis.

2.5. Comparative analysis

The comparative analysis of the 3D-printed copy fidelity was performed using Δs distances between the reference "Artec surface model" and each of the surfaces obtained from the scanning of the respective physical copies. To perform the analysis, Python language was chosen because of its popularity and the large number of available libraries for data analysis. In particular, the following analytic libraries were used:

- *NumPy* (Numerical Python) to support multidimensional massives and their processing.
- *Pandas* – data processing and analysis, CSV file I/O.
- *SciPy* – used for scientific computing and data visualization, especially its "stats" component for probability distributions, summary and frequency statistics, correlation functions and statistical tests.
- *Matplotlib and Seaborn* – enabled to produce plots and statistical graphics.

Kaggle platform, a subsidiary of Google LLC, was found as an appropriate environment for the analysis. Kaggle is an online community of data scientists and machine learning practitioners. The platform allows its users to find and publish their data sets, as well as to explore and build relevant models in a web-based data-science environment. Moreover, users can work with other scientists and engineers, in terms of data processing and machine learning, and solve challenges typical for data science.

Initial data for the current research were as follows:

- Triangulated 3D models obtained from scanning the additively manufactured copies of *Madygenerpeton* fossil skull listed in Table 1.
- Calculated distances between the reference triangulated digital model used for additive manufacturing (3D printing) of the copies and the digital models obtained from scanning these copies [28].

The analysis of distances Δs between the reference "Artec surface model" and each 3D-printed copy of *Madygenerpeton* fossil skull first consisted of the minimization of the distances between two digital surfaces based on 2000 points. Further, detailed statistical analysis of the preliminary data was performed using the CAD system PowerShape (by Autodesk) and

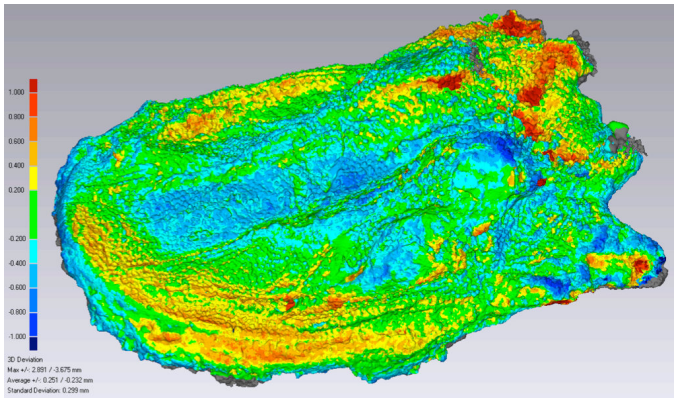

Fig. 4. Example of a colored map of Δs distances between reference digital surface "Artec" and scanning results of copy #7

3D scanning software Geomagic Wrap (3D Systems, Inc.). An example of the distances map is presented in Fig. 4.

The initial database built from the results of distances Δs calculation consisted of 38,866 rows for each copy specified in Table 1.

3. RESULTS AND DISCUSSION

The analyzed fossil skull of *Madygenerpeton* has very complicated surface features. As a result, after the analysis of the measured distances in the PowerShape system, quite a large number of incorrect values appeared. Mainly these incorrect values are related to the uncertain direction of the calculated Δs_i distance between the i-th couple of surface areas. Thus, data filtration was necessary to determine the values exceeding the acceptable limit $\{\Delta d\}_{\max} = \{0.5; 1.0; 1.5; 2.0\}$ mm. As a result, a database was obtained with a number of rows $N = \{13951, 18679, 20820, 22850\}$, dependent on $\{\Delta s\}_{\max}$ value.

3.1. Effect of data filtration limits

In order to assess the effect of different $\{\Delta s\}_{\max}$ values on the final results, several varying values were chosen. This approach allowed for a better understanding of the impact of the filtration method on the obtained static characteristics. Moreover, it helped obtain reasonably justified $\{\Delta s\}_{\max}$ value for the most probable distances Δs.

Trends of the dependence of statistical characteristics on the data filtration are presented in Fig. 5. Statistical characteristics were determined for the modules since the direction of the distance between the analyzed surface and the reference model does not matter.

The diagrams in Fig. 5 demonstrate that the decrease of $\{\Delta d\}_{\max}$ value represented the most distinguishable characteristics in the compared datasets. It can be concluded thus, that the approach was correct. Most interesting are the results obtained for $\{\Delta d\}_{\max} = 0.5$ mm because it may be derived from the industrial experience that the geometrical deviations of the produced objects from the designed 3D surface usually do not exceed 0.5 mm. Moreover, from the methodological perspective, it is important to analyze the results obtained for $\{\Delta s\}_{\max} = 1.0$ mm as well.

The results of the statistical analysis of distances Δs for the examined datasets are shown in Table 2. These datasets correspond with respective 3D-printed copies of the fossil skull and the filtration limits $\{\Delta d\}_{\max} = \{0.5; 1.0\}$ mm.

The analysis of the statistical characteristics of Δs distances presented in Table 2 shows significant differences in mean values $\{\Delta s\}_{\text{mean}}$ between 0.067 and 0.214 for $\{\Delta d\}_{\max} = 0.5$ mm, while the standard deviations are quite similar. For most of the datasets, it was $\sigma \in [0.056; 0.089]$ and the variation coefficient was $v_\sigma \in [0.020; 0.035]$. Only two datasets, corresponding to copies #1 and #7, differed considerably. Here, $\sigma \in [0.134; 0.137]$ and the variation coefficient was $v_\sigma \in [0.108; 0.112]$, i.e. some 3 or even 5 times larger distributions than for other datasets.

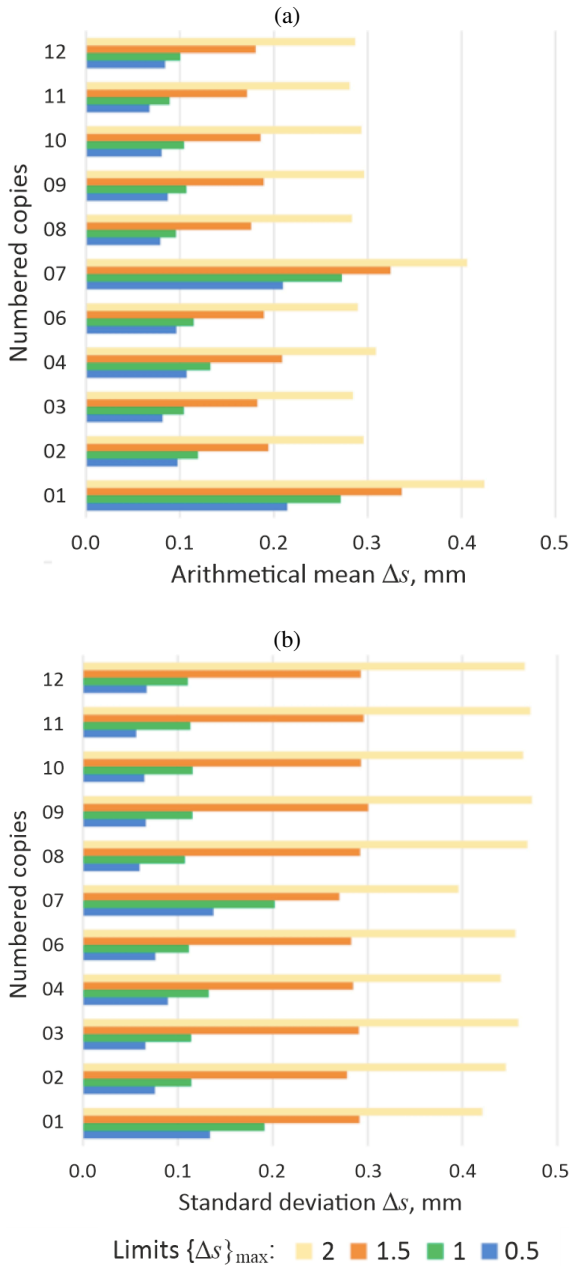

Fig. 5. Effect of the limits of $\{\Delta s\}_{\max}$ values set during the data filtration on the statistical characteristics of Δs values distribution

Table 2
Results of the statistical analysis of distances Δ between the reference model and measured surfaces of the respective copies

No.	$\{\Delta s\}_{\max}$ mm	Distance statistics				
		Mean	Standard deviation	Quartile 25%	Median 50%	Quartile 75%
#1	1.0 0.5	0.271 0.214	0.191 0.134	0.118 0.101	0.238 0.202	0.390 0.317
#2	1.0 0.5	0.119 0.097	0.114 0.076	0.044 0.038	0.093 0.081	0.160 0.139
#3	1.0 0.5	0.104 0.082	0.114 0.066	0.035 0.031	0.076 0.067	0.135 0.116
#4	1.0 0.5	0.132 0.107	0.132 0.089	0.043 0.037	0.098 0.084	0.179 0.156
#6	1.0 0.5	0.115 0.096	0.112 0.076	0.040 0.036	0.088 0.079	0.155 0.138
#7	1.0 0.5	0.273 0.210	0.202 0.137	0.109 0.090	0.236 0.193	0.395 0.317
#8	1.0 0.5	0.096 0.079	0.107 0.060	0.034 0.032	0.072 0.067	0.123 0.112
#9	1.0 0.5	0.107 0.087	0.115 0.066	0.039 0.036	0.081 0.074	0.136 0.123
#10	1.0 0.5	0.104 0.080	0.115 0.065	0.035 0.030	0.076 0.065	0.135 0.115
#11	1.0 0.5	0.089 0.067	0.113 0.056	0.027 0.024	0.062 0.055	0.109 0.097
#12	1.0 0.5	0.100 0.084	0.110 0.067	0.033 0.031	0.075 0.070	0.132 0.121

The obtained results are mostly in agreement with the previous ones described in [26]. Thus, among the best copies of the examined fossil skull can be found #11, #10, #3, and #12, in the order from the best to the worst. They were represented by the smallest values of the main statistical parameters. In turn, copies #7 and #1 can be considered the ones with the largest deviations from the original fossil skull.

3.2. Analysis of Δs distributions

Figure 6 presents a "Box Whiskers" visualization of the comparative analysis of Δs distribution for $\{\Delta s\}_{\max} = 1.0$ mm. It also confirms the previous selection of the best and the worst copies for the filtration limits $\{\Delta d\}_{\max} = \{0.5; 1.0\}$ mm. Hence, the approach to the data filtration and the correctness of filtration limits $\{\Delta d\}_{\max}$ were affirmed.

The visual analysis of the examined datasets of Δs shown in Fig. 6 allowed for the confirmation of the earlier rating of the best and worst copies independently of the chosen filtration limits $\{\Delta d\}_{\max} = \{0.5; 1.0\}$ mm. Thus, it can be assumed that the proposed approach was correct and limits wer chosen properly.

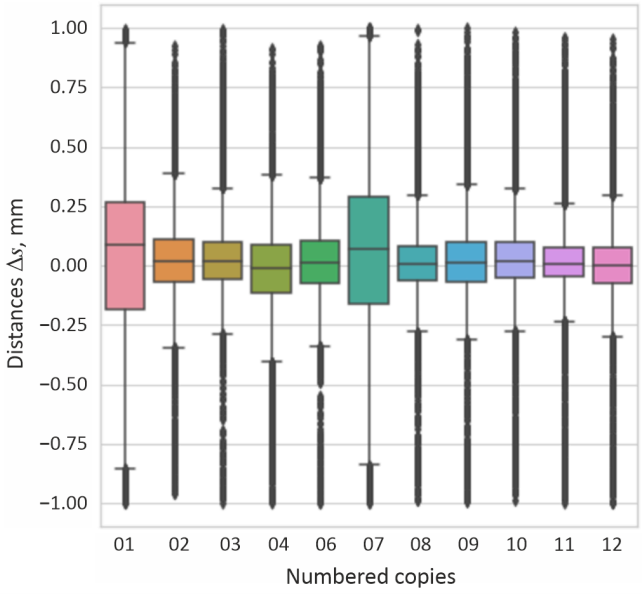

Fig. 6. Comparative statistical analysis of distances Δs between the reference model and the respective copies at $\{\Delta s\}_{\max} = 1.0$ mm

3.3. Correlation analysis of Δs distributions

Further, correlation analysis was performed in order to detect possible dependences of the calculated distances Δs for all possible combinations of 3D-printed copies. Visualization of the analysis in respect of the correlation coefficient is presented in Fig. 6.

Analysis of the correlations shown in Fig. 7 revealed small values of the coefficients r for most of the couples of datasets. However, there are some exceptions, namely for couples #8–#9 and #8–#11 the value of $r = 0.77$, as well as for #6–#8 and #8–#12 the value of $r = 0.76$. Generally, correlation lays in the range $r \in [0.07; 0.77]$. When its value is small, $r < 0.75$, it indicates a weak correlation between the surfaces and, hence, substantial differences between the compared 3D models. When $r < 0.50$, it can be stated that there is no correlation between the distances Δs.

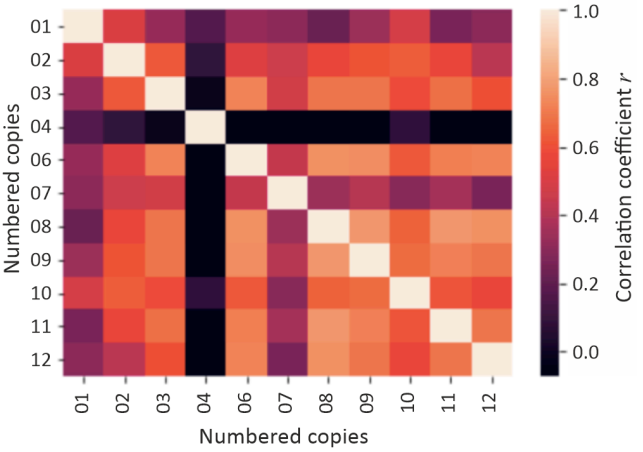

Fig. 7. Correlation coefficients for distances Δs between the reference model and the respective copies between the distances Δs

3.4. Form of Δs distributions

The form of the distribution of the obtained distances Δs was also taken into consideration. In the analysis, data on the Δs distances was taken from the records of comparative analysis results performed in the PowerShape program. Figures 8–12 illustrate the histograms of Δs distributions. In Fig. 8, all the obtained results are presented together, while in Figs. 9 and 10 the best results are shown, obtained for copies #11 and #10, respectively. In contrast, Figs. 11 and 12 show the histograms for the worst models, #7 and #1, respectively.

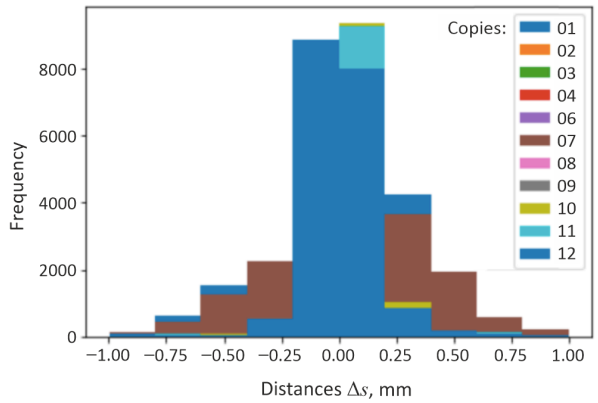

Fig. 8. Histogram of distributions of Δs for all copies, considering also directions

Visualization of Δs distributions for all the copies brought together in one histogram helps to analyze the results and illustrate the common features. It can be observed that for all analyzed copies, the majority of the differences lay in an interval of $\Delta \in [-0.30; 0.40]$ which corresponds to most of the surface of the fossil skull. In fact, between 70% and 90% of the measuring points belonged to this interval with an average ca. 92%.

When all the results are analyzed, the statistical average of the distances is positive (in plus) and has a value $\overline{\Delta s} = 0.190$ mm. The particular averages $\overline{\Delta s_i}$ for the copies were all in an interval $[-0.021; 0.055]$. Thus, the statistical distribution of averages is biased toward positive values of distances Δs from the reference model. In fact, this observation remains in conformity with the previous experience with AM technologies concerning the linear dimensions of simple 3D-printed shapes. Hence, the obtained results indicate no excessive error or wrong metrological approach and the conclusions on the accuracy of the fossil skull 3D copies seem to be reliable.

The histograms for the best copies shown in Figs. 9 and 10 are quite similar in their shapes. In the same way, the histograms for the worst copies seen in Figs. 11 and 12 exhibit apparent similarity. These results provided further evidence for the correct classification of the respective 3D-printed copies in their relation to the reference digital surface. The expanded results of the statistical analysis of the investigated datasets, including tests, can be found on the specialized Kaggle website under the following link: https://www.kaggle.com/code/yaroslavgaraschchenko/notebook-3d-models-fossil-skull-2022-04-30.

The obtained results can be considered an initial stage of the comparative analysis of the feasibility of AM technology to reproduce important geometrical features of the examined fossil skull. The analysis provided some metrological ground for the proper choice of the AM technique in order to ensure the required reproduction of surface texture and dimensional accuracy of the examined object. The issue is highly dependent on the applied technology and material used. Moreover, in AM technology, it is difficult to obtain equally high accuracy throughout the entire reproduced surface. In fact, the large variety of the available 3D printing techniques with essentially different shaping principles and material properties requires a detailed analysis of not only the simple elements [29] but also complex surfaces like the one of *Madygenerpeton* fossil skull.

Thus, forthcoming research should involve more AM techniques and materials as well as different side parameters such as the availability of the device, replicability of results, fabrication time, material costs, long-term usability of the product, etc. Furthermore, a parameter not specifically considered in the frame of this study but generally important for the replication of fossils is coloration. Distinguishable colors are necessary to reproduce the original appearance and are helpful for the recognition of details, especially in scientific research. In practice, 3D-printed copies can be colored by hand or printed in color directly. Among the highest-rated copies, #3 was printed in plain

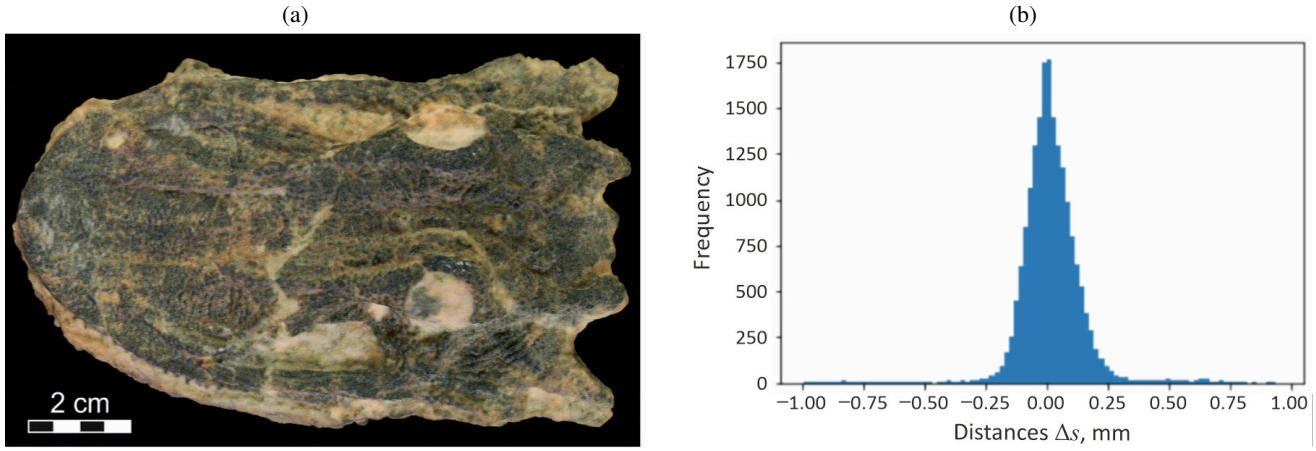

Fig. 9. Copy #11: view (a) and histogram of distributions of Δs (b)

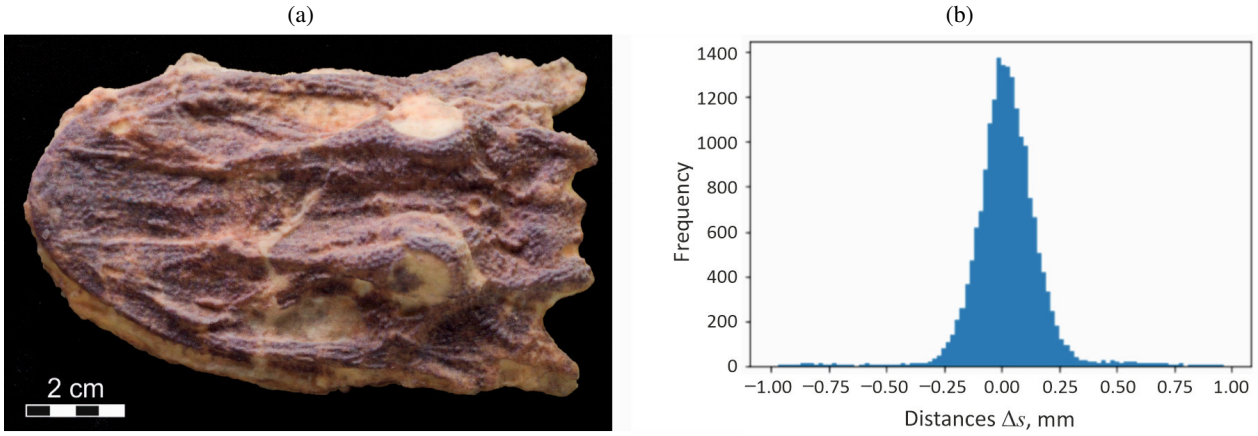

Fig. 10. Copy #10: view (a) and histogram of distributions of Δs (b)

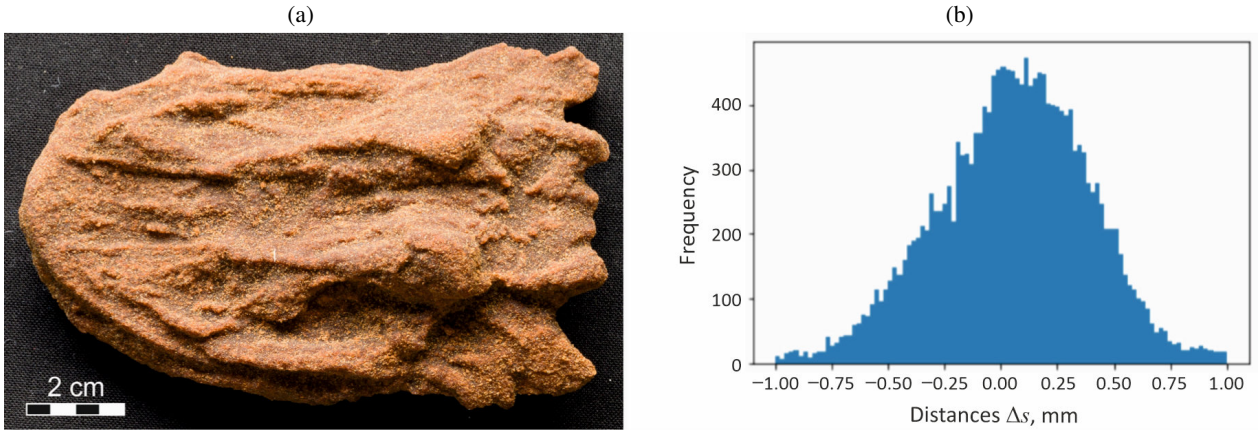

Fig. 11. Copy #7: view (a) and histogram of distributions of Δs (b)

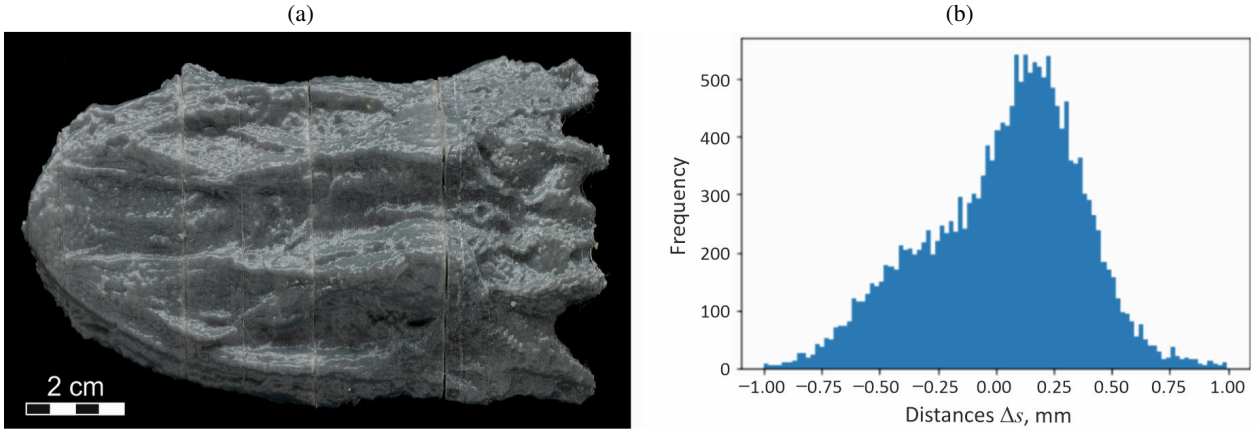

Fig. 12. Copy #1: view (a) and histogram of distributions of Δs (b)

white, while #8 – #12 were produced by color printing. In other words, the quality of the color reproduction should be one of the factors when choosing the suitable technology for the replication of fossils.

Another question to be addressed is the quality of 3D-printed copies depending on the fidelity of the digital 3D model from which it was fabricated. As discussed earlier in [24], the model obtained with the more expensive AICON device is considered more precise than the model generated by the handheld Artec scanner. However, the accessibility and user-friendliness of this latter device still make it an attractive alternative. The extent of deviations between 3D prints from models generated with both machines might further influence the choice of digitization technology.

4. CONCLUSIONS

The results of the performed analysis proved that all the 3D-printed copies of the fossil skull fitted to the tolerance zone of ±0.4 mm for most of its surface. However, considering the small dimensions of the object and its complex surface with numerous small details, it is necessary to set higher requirements for fabrication fidelity.

The analysis of the distances Δs between the reference "Artec surface model" and each of the surfaces obtained from the scanning of the respective 3D-printed copies was performed.

Its results indicated that some copies fitted the tolerances ±0.15 mm for more than 75% of its surface. In particular, copies #3 and #8–#12 met this condition. Copy #11 was found to be the closest to the reference digital model. It can be concluded that among the tested additive manufacturing techniques and materials, #11 allowed for the highest fidelity in the reproduction of the *Madygenerpeton* fossil skull throughout its entire surface. In future research, more AM techniques and materials can be involved in the comparative analysis, including different process parameters.

ACKNOWLEDGEMENTS

The paper was presented and discussed at the International Conference Manufacturing-2022, Poznan, Poland, in May 2022. Results presented in this paper were achieved in the frame of the ESF-funded young researcher group "G.O.D.S." (Geoscientific Objects Digitization Standards) at the TU Bergakademie Freiberg and contributed to the project "When Chemnitz lay on the equator" at the Museum für Naturkunde Chemnitz, Germany. Access to the holotype specimen of *Madygenerpeton pustulatum* was provided by the collection keeper Birgit Gaitzsch (Freiberg, Germany). Alexander Schmiedel, Diana Klemm, Henning Zeidler (Freiberg, Germany), and Maik Jähne (Dresden, Germany) are thanked for their support in obtaining the 3D copies. Authors express their gratitude to the colleagues who helped with the acquisition of 3D data, in particular, Daniel Eger Passos and Sascha Schmidt (Freiberg, Germany), Maik Jähne, Henrik Alhers and Thomas Reuter (Dresden, Germany), Tomasz Szymański and Robert Długoszewski (Mitutoyo Polska, Wrocław, Poland). Lee W. Janson (Falkirk, Scotland) is thanked for linguistic editing.

New research at the Madygen Lagerstätte, Kyrgyzstan, was possible in the frame of the UNESCO International Geoscience Programme (IGCP) Project 727. Unfortunately, no new remains of *Madygenerpeton* have been found found so far.

The project "When Chemnitz lay on the equator" is developed as part of "dive in. Programme for Digital Interactions" of the Kulturstiftung des Bundes (German Federal Cultural Foundation) with funding from the Federal Government Commissioner for Culture and the Media (BKM) through the NEUSTART KULTUR program.

REFERENCES

[1] R.R. Schoch, S. Voigt, and M. Buchwitz, "A chroniosuchid from the Triassic of Kyrgyzstan and analysis of chroniosuchian relationships," *Zool. J. Linn. Soc.*, vol. 160, pp. 515–530, 2010, doi: 10.1111/j.1096-3642.2009.00613.x.

[2] J. Patalas-Maliszewska, R. Wiśniewski, M. Topczak, and M. Wojnakowski, "Design optimization of the Petri net-based production process supported by additive manufacturing technologies," *Bull. Polish Acad. Sci. Tech. Sci.*, vol. 70, no. 2, p. e140693, 2022, doi: 10.24425/bpasts.2022.140693.

[3] X. Zhang, W. Fan, and T. Liu, "Fused deposition modeling 3D printing of polyamide-based composites and its applications," *Compos. Commun.*, vol. 21, p. 100413, 2020, doi: 10.1016/j.coco.2020.100413.

[4] J. Woźniak, G. Budzik, Ł. Przeszłowski, and K. Chudy-Laskowska, "Directions of the development of the 3D printing industry as exemplified by the polish market," *Manag. Prod. Eng. Rev.*, vol. 12, no. 2, pp. 98–106, 2021, doi: 10.24425/mper. 2021. 137682.

[5] J. Gardan, "Additive manufacturing technologies: state of the art and trends," *Int. J. Prod. Res.*, vol. 54, no. 10, pp. 3118–3132, 2016, doi: 10.1080/00207543.2015.1115909.

[6] H. Elhoone, T. Zhang, M. Anwar, and S. Desai, "Cyber-based design for additive manufacturing using artificial neural networks for Industry 4.0," *Int. J. Prod. Res.*, vol. 58, no. 9, pp. 2841–2861, 2020, doi: 10.1080/00207543.2019.1671627.

[7] Y. Wang, Y. Lin, R.Y. Zhong, and X. Xu, "IoT-enabled cloud-based additive manufacturing platform to support rapid product development," *Int. J. Prod. Res.*, vol. 57, no. 12, pp. 3975–3991, 2019, doi: 10.1080/00207543.2018.1516905.

[8] M. Rosienkiewicz, J. Gabka, J. Helman, A. Kowalski, and S. Susz, "Additive manufacturing technologies cost calculation as a crucial factor in industry 4.0," in *Advances in Manufacturing. Lecture Notes in Mechanical Engineering*, A. Hamrol, O. Ciszak, S. Legutko, and M. Jurczyk, Eds., Cham: Springer, 2018, pp. 171–183, doi: 10.1007/978-3-319-68619-6_17.

[9] E. Tsirogiannis, and G. Vosniakos, "Redesign and topology optimization of an industrial robot link for additive manufacturing," *Facta Univ. Ser. Mech. Eng.*, vol. 17, no. 3, pp. 415–424, 2019, doi: 10.22190/FUME181219003T.

[10] R. Singh *at al.*, "Powder bed fusion process in additive manufacturing: an overview," *Mater. Today: Proc.*, vol. 26 (Part 2), pp. 3058–3070, 2020, doi: 10.1016/j.matpr.2020.02.635.

[11] M. Schneck, M. Horn, M. Schmitt, C. Seidel, G. Schlick, and G. Reinhart, "Review on additive hybrid- and multi-material-manufacturing of metals by powder bed fusion: state of technology and development potential," *Prog. Addit. Manuf.*, vol. 6, no. 4, pp. 881–894, 2021, doi: 10.1007/s40964-021-00205-2.

[12] I. Gibson, D. Rosen, B. Stucker, and M. Khorasani. *Additive Manufacturing Technologies*. 3rd edn., Cham: Springer, 2021, doi: 10.1007/978-3-030-56127-7.

[13] J.W. Adams, A. Olah, M.R. McCurry, and S. Potze, "Surface model and tomographic archive of fossil primate and other mammal holotype and paratype specimens of the Ditsong National Museum of Natural History, Pretoria, South Africa," *PLoS One*, vol. 10, no. 10, p. e0139800, 2015, doi: 10.1371/journal.pone.0139800.

[14] A.J. Das, D.C. Murmann, K. Cohrn, and R. Raskar, "A method for rapid 3D scanning and replication of large paleontological specimens," *PLoS ONE*, vol. 12, no. 7, p. e0179264, 2017, doi: 10.1371/journal.pone.0179264.

[15] W. Gao *et al.*, "The status, challenges, and future of additive manufacturing in engineering," *Comput.-Aided Des.*, vol. 69, pp. 65–89, 2015, doi: 10.1016/j.cad.2015.04.001.

[16] L. Di Angelo, P. Di Stefano, and E. Guardiani, "Search for the optimal build direction in additive manufacturing technologies: A review," *J. Manuf. Mater. Process.*, vol. 4, no. 3, p. 71, 2020, doi: 10.3390/jmmp4030071.

[17] E. Dalpadulo, F. Pini, and F. Leali, "Assessment of design for additive manufacturing based on CAD platforms," in *Proc.s of International Conference on Design, Simulation, Manufacturing: The Innovation Exchange*, Cham: Springer, 2019, pp. 970–981.

[18] Y. Zhang, Y. Xu, and A. Bernard, "A new decision support method for the selection of RP process: knowledge value measuring," *Int. J. Comput. Integr. Manuf.*, vol. 27, no. 8, pp. 747–758, 2014, doi: 10.1080/0951192X.2013.834474.

[19] A. Razavykia, E. Brusa, C. Delprete, and R. Yavari, "An overview of additive manufacturing technologies – A review to technical synthesis in numerical study of selective laser melting," *Materials*, vol. 13, no. 17, p. 3895, 2020, doi: 10.3390/ma13173895.

[20] L. Di Angelo, P. Di Stefano, and A. Marzola, "Surface quality prediction in FDM additive manufacturing," *Int. J. Adv. Manuf. Technol.*, vol. 93, no. 9, pp. 3655–3662, 2017, doi: 10.1007/s00170-017-0763-6.

[21] H. Chen, and Y.F. Zhao, "Process parameters optimization for improving surface quality and manufacturing accuracy of binder jetting additive manufacturing process," *Rapid Prototyping J.*, vol. 22, no. 3, pp. 527–538, 2016, doi: 10.1108/RPJ-11-2014-0149.

[22] N. Li *et al.*, "Progress in additive manufacturing on new materials: A review," *J. Mater. Sci. Technol.*, vol. 35, pp. 242–269, 2019, doi: 10.1016/j.jmst.2018.09.002.

[23] S. Voigt *et al.*, "Triassic life in an inland lake basin of the warm-temperate biome – the Madygen Lagerstätte (southwest Kyrgyzstan, Central Asia)," in *Terrestrial conservation Lagerstätten. Windows into the evolution of life on land*, N.C. Fraser, H.D. Sues, Eds., Edinburgh, London: Dunedin, 2017, pp. 65–104.

[24] Ya. Garashchenko, I. Kogan, and M. Rucki, "Comparative accuracy analysis of triangulated surface models of a fossil skull digitized with various optic devices," *Metrol. Meas. Syst.*, vol. 29, no. 1, pp. 37–51, 2022, doi: 10.24425/mms.2022.138547.

[25] Ya. Garashchenko, I. Kogan, and M. Rucki, "Analysis of 3D triangulated models of *Madygenerpeton pustulatum* fossil skull," in *Proc. euspen's 21st International Conference & Exhibition*, 2021, pp. 89–90.

[26] M., Rucki, Y., Garashchenko, I., Kogan, and T. Ryba, "Evaluation of the Fidelity of Additively Manufactured 3D Models of a Fossil Skull," in: *Advances in Manufacturing III. MANUFACTURING 2022. Lecture Notes in Mechanical Engineering*. M. Diering, M. Wieczorowski, M. Harugade, A. Pereira, Eds., Cham: Springer, 2022, pp. 36–47, doi: 10.1007/978-3-031-03925-6_4.

[27] I. Kogan, M. Rucki, M. Jähne, D. Eger Passos, T. Cvjetkovic, and S. Schmidt, "One head,many approaches – comparing 3D models of a fossil skull," in *Photogrammetrie – Laserscanning – Optische 3D-Messtechnik: Beiträge der Oldenburger 3D-Tage 2020*. T. Luhmann, C. Schumacher, Eds., Berlin: Wichmann Verlag, 2020, pp. 22–31.

[28] M. Rucki, I. Kogan, and Ya. Garashchenko, *Distances between 3D models of a fossil skull*, Dataset. Kaggle, 2022, doi: 10.34740/KAGGLE/DSV/3520649.

[29] M.Á. Caminero, J.M. Chacón, E. García-Plaza, P.J. Núñez, J.M. Reverte, and J.P. Becar, "Additive manufacturing of PLA-based composites using fused filament fabrication: Effect of graphene nanoplatelet reinforcement on mechanical properties, dimensional accuracy and texture," *Polymers*, vol. 11, no. 5, p. 799, 2019, doi: 10.3390/polym11050799.